Impedance spectroscopy study of the retinal pigment epithelium: Application to the monitoring of blue light exposure effect on A2E-loaded in-vitro cell cultures

Jocelyn Boutzen, Manon Valet, Agathe Alviset, Valérie Fradot, Lionel Rousseau, Olivier Français, Serge Picaud, Gaelle Bazin Lissorgues

Impedance spectroscopy study of the retinal pigment epithelium: Application to the monitoring of blue light exposure effect on A2E-loaded in-vitro cell cultures.

Jocelyn Boutzen, Olivier Français, Lionel Rousseau and Gaëlle Lissorgues : ESIEE-Paris, ESYCOM Université Paris-Est, Noisy-le-Grand, 93160, France.

Valérie Fradot, Manon Valet, Agathe Alviset and Serge Picaud : Institut de la Vision, INSERM, CNRS, Sorbonne Université, Paris, 75012, France

Abstract

Impedance spectroscopy study of the retinal pigment epithelium: Application to the monitoring of blue light exposure effect on A2E-loaded in-vitro cell cultures.

Abstract

In age-related macular degeneration, the retinal pigment epithelium can be damaged by light acting on photosensitizers like N-retinylidene-N-retinylethanolamine (A2E). In this paper, the underlying cellular mechanism of lesion at the cell layer scale is analyzed by impedance spectroscopy. Retinal pigment epithelium (RPE) cells are cultured on top of custom-made electrodes capable of taking impedance measurements, with the help of a custom-made electronic setup but without the use of any chemical markers. An incubator is used to house the cells growing on the electrodes. An electrical model circuit is presented and linked to the constituents of the cell layer in which various electrical elements have been defined including a constant phase element (CPE) associated to the interface between the cell layer and the electrolyte. Their values are extracted from the fitted model of the measured impedance spectra. In this paper, we first investigate which parameters of the model can be analyzed independently. In that way, the parameter's evolution is examined with respect to two different targeted changes of the epithelium: 1. degradation of tight junctions between cells by extracellular calcium sequestration with Ethylenediaminetetraacetic acid (EDTA); 2. application of high amplitude short length electric field pulses. Based on the results obtained showing a clear relation between the model and the physiological state of the cell layer, the same procedure is applied to blue light exposure experiment. When A2E-loaded cells are exposed to blue light, the model parameters indicate, as expected, a clear degradation of the cell layer opposed to a relative stability of the not loaded ones.

Keywords

Impedance spectroscopy, Retinal pigment epithelium, Constant Phase Element, Blue light

1. Introduction

In age-related macular degeneration, light exposure was identified as a risk factor [1]. This light mediated damage was attributed to the photosensitization of the retinal pigment epithelium with photosensitizers contained in lipofuscin such as N-retinylidene-N-retinylethanolamine (A2E) [2]. The retinal pigment epithelium (RPE) is a monolayer of epithelial cells lying between the photoreceptor's outer segment and the innermost layer of the choroid called the Bruch's membrane [3]. Like other types of epithelial cells, the RPE cells form tight junctions and provide nutriments to photoreceptors, recycle the visual pigment and phagocyte the tips of oxidized photoreceptor outer segments. As a consequence, lipofuscin and photosensitive derivatives of the visual pigments such as A2E accumulates in these cells during aging within lysosomes [4] [5] [6]. The photosensitization of these derivatives induces oxidative stress resulting in different cell alterations [7] [8] [9].

To further assess these cellular alterations, impedance spectroscopy provides an approach for monitoring conductive and dielectric materials like cells that are kept in close contact to an electrode [10] [11] [12] [13]. It enables investigators to measure the electric dipoles representing cell junctions and cell membranes. The method consists in applying a voltage stimulations of given amplitude in a wide range of frequencies to measure the current response or, alternatively, apply a current while measuring the voltage drop [14]. If the stimulation is small enough to ensure that the system is kept close to its equilibrium point, then the non-linearity (such as electrochemical reactions) can be ignored. One can compute the impedance associated with such a measurement by calculating $\underline{\mathbf{Z}} = \underline{\mathbf{V}}/\underline{\mathbf{I}}$ where $\underline{\mathbf{Z}}$, $\underline{\mathbf{V}}$ and $\underline{\mathbf{I}}$ are complex numbers, $\underline{\mathbf{Z}}$ the impedance, $\underline{\mathbf{V}}$ the measured or applied voltage, and **I** the measured or applied current. The measurement is conducted over a frequency bandwidth to construct the spectrum of the impedance containing the modulus and the phase of the impedance.

From cell suspension [15] [16] [17] to plated cells [18] [19] [20] [21], the application of impedance spectroscopy extends over a wide range of biological systems in-vitro and is also used in-vivo, for instance as a way to characterize an artificial implant interaction's with tissues. The evaluation of the impedance can be done at a fixed frequency, usually 1 kHz [22] [23] for implants, or lower frequencies (around 10 Hz) for instance, to measure the Trans-Epithelial Electrical Resistance (TEER) [24]. When the measurement extends over a large frequency band, the data can also be fitted with an electrical model made of linear dipoles [25].

In the present study, the light induced damage over A2E-loaded RPE cells using impedance spectroscopy is investigated. The measurement is performed using a 10 mVrms amplitude sinusoidal stimulation over a [1 Hz, 1 MHz] bandwidth. Then an electrical model circuit is fitted to the data enabling parameters extraction. A constant phase element (CPE) is used as part of the electric description of the cell layer to take into account the spatial distribution of its capacitance. The physical meaning of such element is subjected to discussions [26] [27] [28]. To ensure that the model's parameters are truly associated with the proposed cell layer components, and in order to investigate if they can be analyzed independently, they have been monitored during two controlled and targeted lesions of the RPE cells: 1. Degradation of cell's tight junctions by chelation of calcium ions using Ethylenediaminetetraacetic acid (EDTA); 2. application of high amplitude short length electric pulses probably inducing disruption and transient electro-permeabilization of the cell membranes. The measurements done with controlled perturbation of the cell layer indicate that it is acceptable to associate the elements of the model to specific components of the cell layer, namely cell membranes and cell junctions. Taking into account these results, the light induced damage over A2E-loaded RPE cells is evaluated using the same procedure of measurement and parameters extraction. Every cell layer having been exposed to blue light, clear distinctions are observed regarding the parameter variations, between A2E-loaded and non-loaded RPE cells.

2. Material and Methods

2.1. Impedance measurement setup

The measurement setup is composed of a spectrometer (EIS: ZIVE SP1 potentiostat) performing the measurement. The spectrometer is associated with a relay board controlled by an electronic card (Raspberry Pi) for multiplexing capabilities. The electronic card also controls the circuit that triggers light activation on the cell cultures. The measurement is done using a 10 mVrms amplitude sinewave stimulation over a [1 Hz, 1 MHz] bandwidth. Unless otherwise stated, ten points per frequency decade were acquired, for a total measurement time of about 2 minutes. A computer running the spectrometer software is used to communicate with it and process the data to be available on an online dedicated server. The server is also used to remotely control the experiments. In order to reduce the noise to a minimum level, the whole setup is shielded by a Faraday cage. A noise study is presented in Supplementary Figure 1 of the supplementary information section. Fifty consecutive measurements of a disk electrode in culture medium have been performed in order to evaluate standard deviation of the measurement setup. For that test, and to reduce the measurement time to a minimum, only 5 points have been recorded per frequency decade. As seen on the Supplementary Figure 1, the error bar's width would not be visible on the spectra therefore we have not included them on the measurements shown in the paper.

2.2. Device structure

The impedance measurement is performed on a device that includes four identical cell chambers (Figure 1 A and B). At the base of each cell chamber, the device contains platinum electrodes that were produced using a standard lift-off microfabrication process, on a 500 µm thick glass substrate. SU-8 photoresist is used for metallic line passivation. Each chamber of the device is identical to allow for a multiple experiment and/or control procedure. A custom mold is 3D printed to cast a four well PDMS structure used to separate between the four corners. A tight seal between each corner is evaluated using concentrated phenol red. The electrode design used for the experiments is the disk electrode presented Figure 1 C. The diameter of the disk is 1.88 mm and the spacing with the reference electrode is 100 µm. The reference electrode's surface is 13 times bigger than the disk electrode and its influence on impedance can be neglected in what follows. Even if the four disk electrodes on each device are designed identical, technological variations induce a slight spread between them. We evaluated this spread in Supplementary Figure 2 of the supplementary information section. This slight spread was considered acceptable.
For blue light exposure experiments, the LED mount is located 60 mm above the cell layer. A schematic representation of this is shown Figure 1 D. When the EDTA experiment is ongoing, the LED mount and diaphragm are replaced by a pipette tip support. This allows for fast culture medium changes without device disconnections as represented on Figure 1 E. Therefore the procedure involved in manually replacing the culture medium with an EDTA loaded medium in one chamber of the device takes less than 20 seconds.

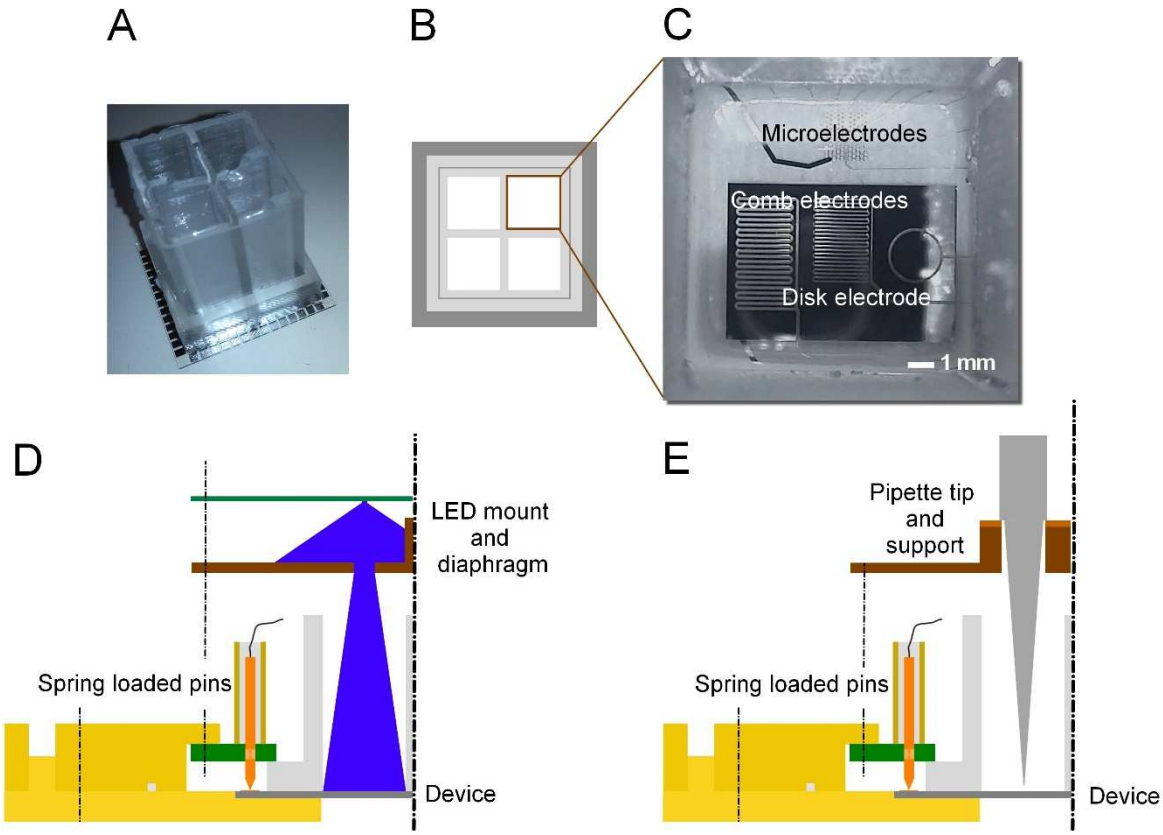

Figure 1 A full device (A), side is about 36 mm. Drawing of the top view of a device (B) and photography of one of the four identical chambers of the device (C). Schematic half-view representations (not to scale) of the device's support with LED mount (D) and pipette tip support (E).

2.3. Cell culture procedure

The RPE cells are extracted from porcine eyes harvested from a local slaughterhouse and detached from the eyecup using trypsin treatment. Slaughterhouse supply allows for the suppression of animal sacrifice in the sole purpose of our experimentations, in accordance with ethical EU recommendations. After counting, cells are seeded in each chamber at a concentration of 300.000 cells per chamber in Dulbecco's Modified Eagle Medium (DMEM) with 20 % fetal calf serum (FCS). For the light exposure experiment, the culture medium used is composed of modified DMEM with no phenol red and a reduced FCS concentration of 10 %. Prior to the seeding and to enhance cell adhesion to the substrate, every chamber is incubated with pure FCS for at least 2 hours. Right after seeding, the device is placed inside a 37 °C, 5 % CO_2 incubator where the whole measurement procedure is conducted. Medium is changed at day 1 to remove cells that would not have attached to the surface.

2.4. Perturbation by EDTA

EDTA solution is prepared with an EDTA disodium salt powder (Sigma-Aldrich) at a concentration of 2.2 mM in the culture medium. The solution is left to stabilize inside the incubator's atmosphere and temperature before the experiment. EDTA is known to interfere with the cell tight junctions by sequestration of calcium ions. Perturbation of cell-cell interaction is happening as a result through actin filaments depolymerization [12]. The EDTA solution is added and measurements are immediately started. This experiment was done 3 times on different cell cultures at confluence.

2.5. Perturbation by high amplitude-short length electric pulses

The electric pulse perturbation consists of ten identical pulses, each of them applied at a one second interval. A pulse has a biphasic shape with a half period of 100 µs. The pulse's amplitude is ± 8 V. Due to the planar electrode's geometry the electric field generated is highly inhomogeneous. The electric field norm estimated with Finite Element Method (Comsol ©) in a plane 5 µm above the electrode's surface is 500 V/cm in a point between electrode and reference, and rises up to 1.38 kV/cm closer to the electrodes. The simulations can be seen on Supplementary Figure 4 of the supplementary material section of this article. This range of electric field in combination with the pulse length is compatible with membrane perturbation leading to transient permeabilization of cell membranes (reversible electroporation) [29].
Immediately after the pulses, the first impedance measurement is taken. This experiment was done 4 times on different cell cultures at confluence. In the experiment, and in order to reduce measurement time, five points per frequency decade are recorded, for a measurement time of about 1 minute.

2.6. A2E incubation procedure

A2E incubation is conducted after the cell layer has reached confluence. In our case, this happens in less than a week and the A2E was incubated at day 10. A2E is incubated for 6 hours with a concentration of 20 µM in culture medium as previously done in [30]. The device is not measured during incubation time. After incubation, a phenol red free version of the DMEM is used with a reduced FCS concentration of 10 % to enhance transparency of the culture medium.

2.7. Blue light exposure characteristics

When light exposure is the ongoing experiment, a LED mount and diaphragm are set on top of the device and the LEDs shine four squares of light on top of the four chambers as represented on Figure 1 D. Using a spectrometer (Jaz, Ocean Optics), irradiance was measured to be 0.6 mW/cm² in the plane of the cell culture and in continuous shining mode. The peak wavelength was also measured to be 430 nm with full width at half maximum of ± 15 nm. The measurement done is shown on Supplementary Figure 3 of the supplementary information section. This is among the

most toxic wavelengths of blue lights [30]. However, to avoid culture heating, the LEDs are triggered with a 1 s period, 25 % duty cycle therefore the average irradiance is 0.15 mW/cm².

3. Results

3.1. The electrical circuit model and the reconstructed capacitance parameter

The electrical circuit model is made of electric dipoles that are associated with different part of the cell layer. It is presented in the inset Figure 2 A. The inset Figure 2 B shows two measured impedance spectra corresponding to single impedance measurements done on culture medium (diamonds) or on confluent cell layer (circles). The associated fitting curves are shown as continuous lines. A schematic representation of the cell layer with corresponding location of the electrical elements of the model is shown Figure 2 C. In this simplified circuit model, a CPE is associated to the electrode-electrolyte interface (Q_{el}, α_{el}) and to the cell membranes-electrolyte interface $(Q_{cell}, \alpha_{cell})$. In the case of the electrode-electrolyte interface, the CPE behavior was suggested to arise from a distribution of time constants, originating from a surface energy distribution due to crystalline disorder at the surface of the electrodes [31]. In the case of the cell layer the α_{cell} parameter is assumed to be similarly associated with a surface distribution but of phospholipids, because they are the fundamental building blocks of the isolating layer that is composing the cell membrane.

The resistance R_{med} is associated to the culture medium (electrolyte) and the last two resistances represent on one hand the space between cells R_{junc} (the junction quality) while the other one R_{me} represents the membrane's resistance itself. These last two resistances cannot be distinguished from one another during the performed measurement. As a consequence, the parallel combination of these two resistances is labeled with the name R_{cell}, the cell layer resistance. The intracellular resistance doesn't appear due to its negligible volume as compared to the extracellular one. The parasitic serial inductances due to wires, the parasitic capacitance, and the resistance in parallel are considered negligible over the frequency bandwidth covered by the cells (from 70 Hz to 40 kHz approximately).

Thus, the mathematical expression of the model's impedance is:

$$Z = \frac{1}{Q_{el}(j\omega)^{\alpha_{el}}} + \frac{R_{cell}}{1 + R_{cell}Q_{cell}(j\omega)^{\alpha_{cell}}} + R_{med} \text{ With } R_{cell} = \frac{R_{junc}R_{me}}{R_{junc}+R_{me}}$$

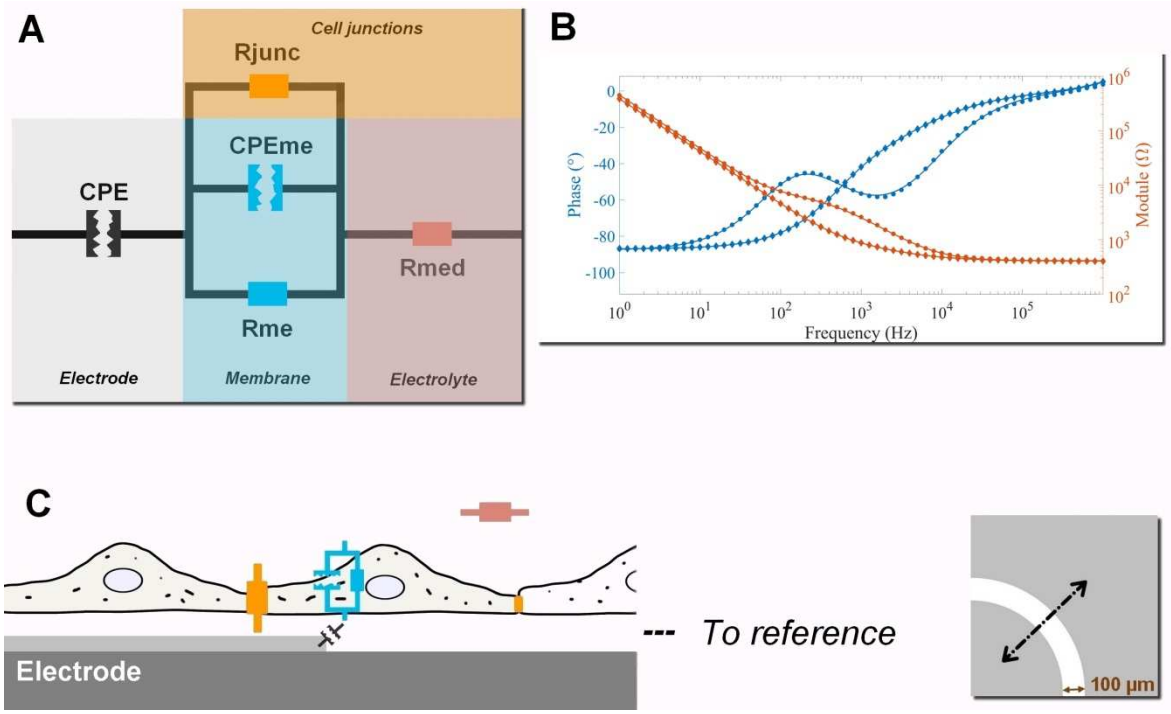

Figure 2 Cut view schematic representation of the cell layer at confluence (C) and associated electrical circuit model (A). The impedance spectrum (B) shows two spectrum measurements and associated fit: With culture medium but no cells (diamonds) and with a cell layer at confluence in culture medium (circles). The measured data are shown with markers only, and the associated fit is the continuous line. All measurements were performed in a Faraday cage to limit noise.

The parameters are extracted using least-square fitting of the model to the data. The fitting is done using Levenberg-Marquardt algorithm from the spectrometer software. Representative examples of the fitting quality are shown in the inset Figure 2 B. In our case the maximum error between data and associated fit over the full frequency bandwidth is 2.48% on the modulus and 1.22° on the phase. Measured data are shown as markers (diamond or circle) and the continuous line represents the fit.

The CPE is often associated with the electrode-electrolyte interface but has also been applied to the modeling of the cell membrane-electrolyte interface [28]. However, the CPE cannot be directly associated with a capacitance and the physical signification or universality of the CPE parameters and behavior are usually unclear.

A reconstructed effective capacitance parameter for the cell membrane with Farad unit is sometimes used instead [28], [25]. For the CPE associated with the cell layer it is defined as:

$$C_{eff} = Q_{cell}^{\frac{1}{\alpha_{cell}}}\left(R_{med}^{-1} + R_{cell}^{-1}\right)^{\frac{\alpha_{cell}-1}{\alpha_{cell}}}$$

This originates from [27] where this procedure was initially presented to describe electrode-electrolyte interface. In our experiments, this reconstruction method is applied to the in-plane surface distributions of time constants [32] that constitute the cell layer.

This effective capacitance is related to the main relaxation time constant in this distribution, retrieved from the maximum of the imaginary part of the admittance. This is the only relaxation time constant that the system would have had if the α_{cell} parameter was unity. Therefore, the effective capacitance is the value of Q_{cell} when $\alpha_{cell} = 1$. If the cell layer brings an inhomogeneous distribution of time constants, as we expect, α_{cell} is no longer unity and the capacitance is no longer Q_{cell} but the previous expression, C_{eff}.

After extraction of the electrical circuit model parameters using the EIS fitting software, the data are analyzed using Matlab (©) in order to calculate the effective capacitance C_{eff}.

C_{eff} represents the cell layer's average capacitance and α_{cell} its distribution. It's not so clear concerning the physical meaning of the parameter Q_{cell}. One can only suggest hypothesis on Q_{cell} significance. However, investigation were conducted to highlight the independence between Q_{cell} and R_{cell}. In that way, EDTA assay (targeting cells junctions) and pulse assay (targeting cells membranes) were conducted. Provided those tests, a dynamic observation of parameter variation is obtained when a specific constituent of the cell layer is being targeted. This gives insight on the physical significance of the model's parameter. The EDTA and pulse tests are presented in Figure 4. Afterward, the same experimental procedure has been applied to the experiments involving A2E and blue light.

3.2. EDTA assay

Figure 3 illustrates the effect of a calcium chelation by EDTA (2.2 mM) on the cell morphology. Rapidly (less than 10 minutes), the confluent layer of RPE cells loses its confluence with space forming between cells Figure 3 B. Washing EDTA restores the cell confluence Figure 3 C. When such an experiment (EDTA 2.2 mM) was followed by impedance spectrometry, shortly after addition of the 2.2 mM EDTA solution, a substantial decrease of the R_{cell} parameter, as well as a substantial but delayed variation of $1/Q_{cell}$ and α_{cell} were observed, as seen in Figure 4 A and C. The parameters tend to stabilize toward a lower value.

Overall, the reconstructed parameter $1/C_{eff}$ is considered to stay stable with a maximum increase inferior to 5% (taking into account all trials) with respect to its initial value before EDTA addition. In the case of EDTA perturbation, it is commonly admitted [12], [33] that the sequestration of calcium ions disrupts the cell layer's tight junctions with a concentration around 2 mM. Indeed, during the experiments, a variation of the $\mathrm{R_{cell}}$ parameter is initially observed, followed by a variation of the $(1/Q_{cell}, \alpha_{cell})$ couple. This can be explained as tight junctions being firstly damaged, which leads to the decrease of the $\mathrm{R_{cell}}$ parameter. Then if the actin filament's disruption is prolonged, the cell shape randomly changes within the cell layer. This happens when the tight junction's integrity has decreased below a critical point where they are no longer capable of maintaining the connection between cells at their side. This leads to disruption of the spatial distribution of the phospholipids. However, the cells remain present at the surface of the electrode which accounts for the relatively small variation of $1/C_{eff}$.

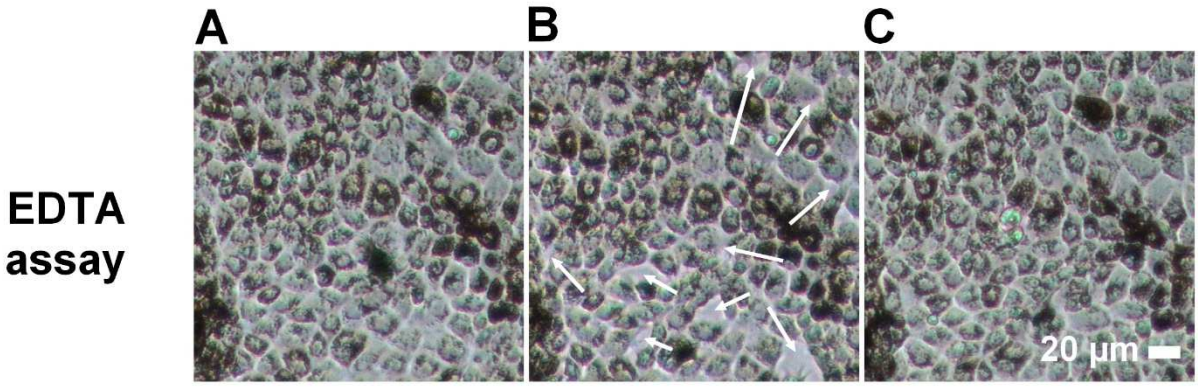

Figure 3 Cells morphology changes upon addition of EDTA (2.2 mM) in the culture medium – same scale on A, B and C.
Image A shows the cell layer prior to EDTA exposition, image B is taken 10 minutes after EDTA exposition and shows profound disruption (see arrows) of the tight junctions leading to cell layer morphology changes. After image B the medium is changed to remove the EDTA. Finally, image C is taken 3h15 after rinsing and corresponds closely to initial image A.

3.3. High amplitude-short length electric pulses

High amplitude electric pulses with short duration are known to produce electroporation in biological membranes [29]. Such pulses are applied on RPE cells to define how such membrane perturbation would affect the impedance spectrum measurement. Immediately after the pulse application, the $1/Q_{cell}$ and α_{cell} parameter values drop together (Figure 4 B and D). This effect is followed by a delayed decrease of R_{cell}. The $1/Q_{cell}$ and α_{cell} parameters then immediately settle back to their initial levels, a few minutes after the pulses, without further manipulations. On the other hand, the R_{cell} parameter takes more time to recover and settles back after several hours. The variations of the reconstructed parameter $1/C_{eff}$ are small compared to the fitted parameters (less than 3% variation). During electroporation, the targeted elements of the cell layer are the membrane's phospholipids which are polar molecules and therefore sensitive to high intensity electric fields. The collective variation of $1/Q_{cell}$ and α_{cell} is associated with the transitory de-homogenization of such phospholipid's position and orientation in the cell membranes of the layer, as a result of the electric field application.

However, the sampling time in between impedance measurement (and therefore in between parameters acquisition), is too long to visualize a transient permeabilization of the cell membrane on the resistance parameter. The $1/Q_{cell}$ variation thus reflects the phospholipids dipolar moments settling back to their unperturbed state. Nevertheless, a delayed variation of R_{cell} is observed which can be interpreted as a perturbation of the tight junctions following the pulses.

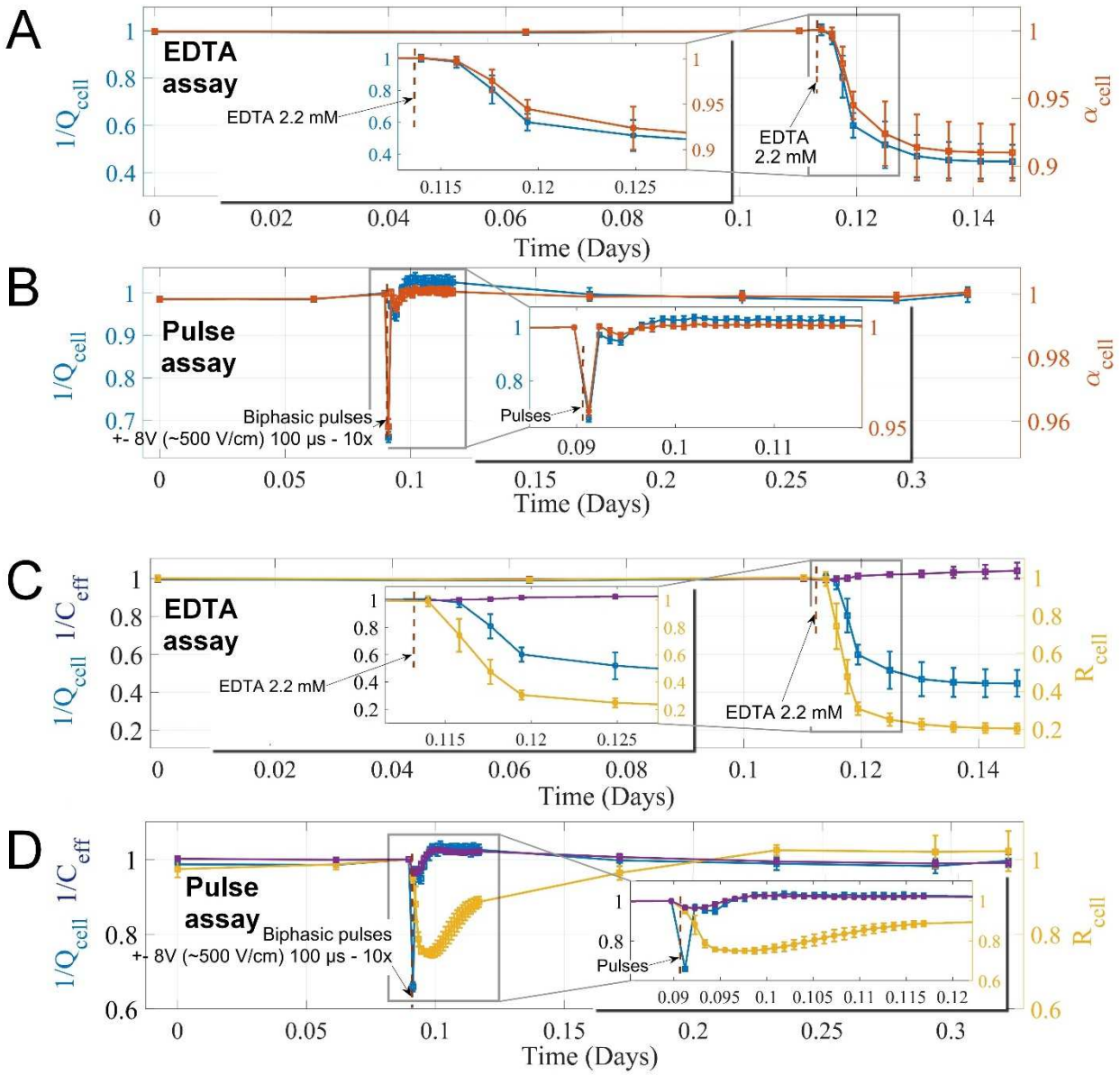

Figure 4 Cell membrane's CPE parameters ($1/Q_{cell}$ in blue and α_{cell} in red) relative variation during EDTA perturbation (A) and electric pulse perturbation (B). Relative variations of R_{cell} (yellow), $1/Q_{cell}$ (blue) and $1/C_{eff}$ (violet), during EDTA perturbation (C) and electric pulse perturbation (D). The parameters are normalized by their value prior to the perturbation in order to compare their relative variations. Data points are showing the mean value of 3 trials (EDTA assay) and 4 trials (Pulse assay). Error bar length indicates standard deviation among trials. Insets are showing a detailed view of the data around the perturbation.

3.4. A2E application and blue light exposure

Based on this preliminary study on the correspondence of the model's parameter with biological components, the same measurement and analysis procedure are applied to the investigation of blue light exposure effect of the A2E-loaded RPE cell layer.

A2E was applied on RPE cells to mimic their ageing. As this A2E application can alter cell function, the variation of the electrical parameters was monitored, prior to the LED light illumination. A2E (20 µM) was applied on two chambers while cells on the other wells were not administered A2E to be used as a reference. In that part of the experiment, the parameter $1/Q_{cell}$ remained stable with a variation of less than 10 % in all chambers. However, the R_{cell} parameter decreased as a consequence of the medium application, but in a significantly higher proportion in chambers receiving A2E.

After a period for parameter stabilization, the LED light was turned on above all chambers. While the control chamber remained stable, the A2E chamber showed a variation in all the $1/Q_{cell}$, $1/C_{eff}$ and R_{cell} parameters. When the light was turned off, all parameters continued to vary. This suggests that the interaction between A2E and blue light is generating by-products that continue to interact with the cells. These major changes were consistent with the microscopic examination of the cells after light exposure Figure 5 B, D and F. Indeed, following A2E application and light exposure, cell junctions were no longer clearly distinguished suggesting significant tissue damage. Upon cell medium replacement, all parameters slowly recovered to their initial values.

From analysis of the two perturbations (EDTA, Pulses), it can be considered that the parameter $\mathrm{R_{cell}}$ reflects the cell junctions quality, parameters $1/\mathrm{Q_{cell}}$ and α_{cell} are associated to the cell membrane's phospholipids distribution and the reconstructed element $1/\mathrm{C}_{eff}$ its average capacitance value.

As for the A2E and blue light assay, two steps were observed. During the first step, which corresponds to the pre-illumination period indicated on Figure 6, the A2E has been incubated in two of the device's corners but the light has not been turned on yet. During that time (Figure 6 A), a variation of the $\mathrm{R_{cell}}$ parameter is observed in the three wells but in a significantly higher proportion in the two wells that received A2E (- 1259 Ω and -1018 Ω corresponding to – 47 % and – 41 %) as opposed to the well that did not receive A2E (-254 Ω corresponding to -11 %), with respect to the value recorded prior to A2E incubation. The $1/Q_{cell}$ and $1/C_{eff}$ variations during the pre-illumination period (Figure 6 B, C) were small and not discriminable between wells that received A2E or not. Therefore, by comparison with the beginning of the EDTA assay, it can be concluded that A2E incubation (20 µM) has an effect on the tight junctions but not on the membrane integrity.

During the second step of the A2E and blue light assay, the light was turned on. At that point, it is clear in Figure 6 that the chambers which received A2E see their parameters varying in a more significant manner when exposed to blue light. This differs from the control chamber which received blue light but no A2E. In the chambers that received A2E, $1/C_{eff}$ variations on Figure 6 C are analyzed as a destruction of the cell layer that is confirmed by the images shown on Figure 5

C, D and E, F. When the light is turned off, the parameters $1/Q_{cell}$ and $\mathrm{R_{cell}}$ settle back after one day.

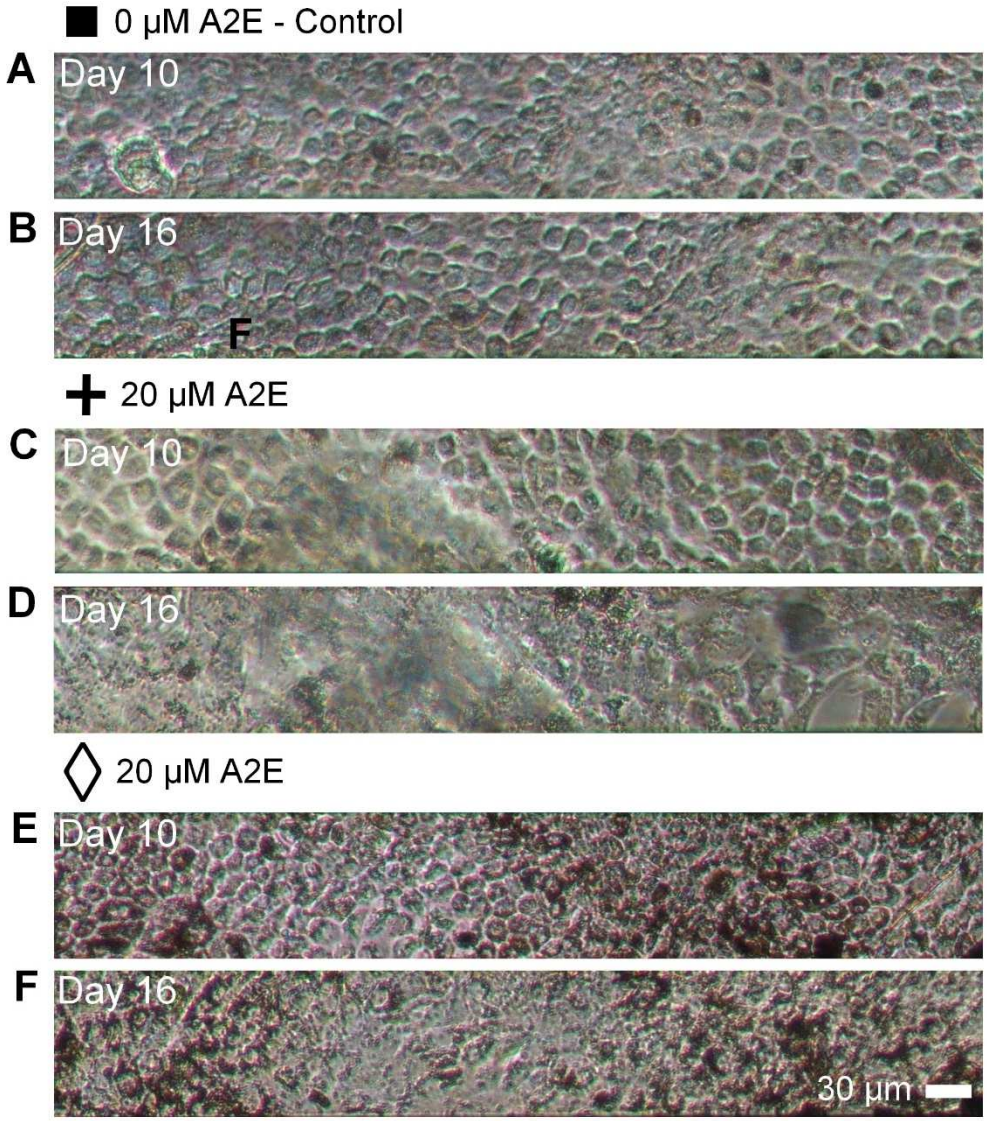

Figure 5 Cell culture before and after the blue light assay. Images were taken at day 10 (before A2E incubation) and at day 16 before culture medium replacement (but after light exposure between day 12 and day 14). Symbols on the image next to the A2E concentration are referring to the symbols used in Figure 6

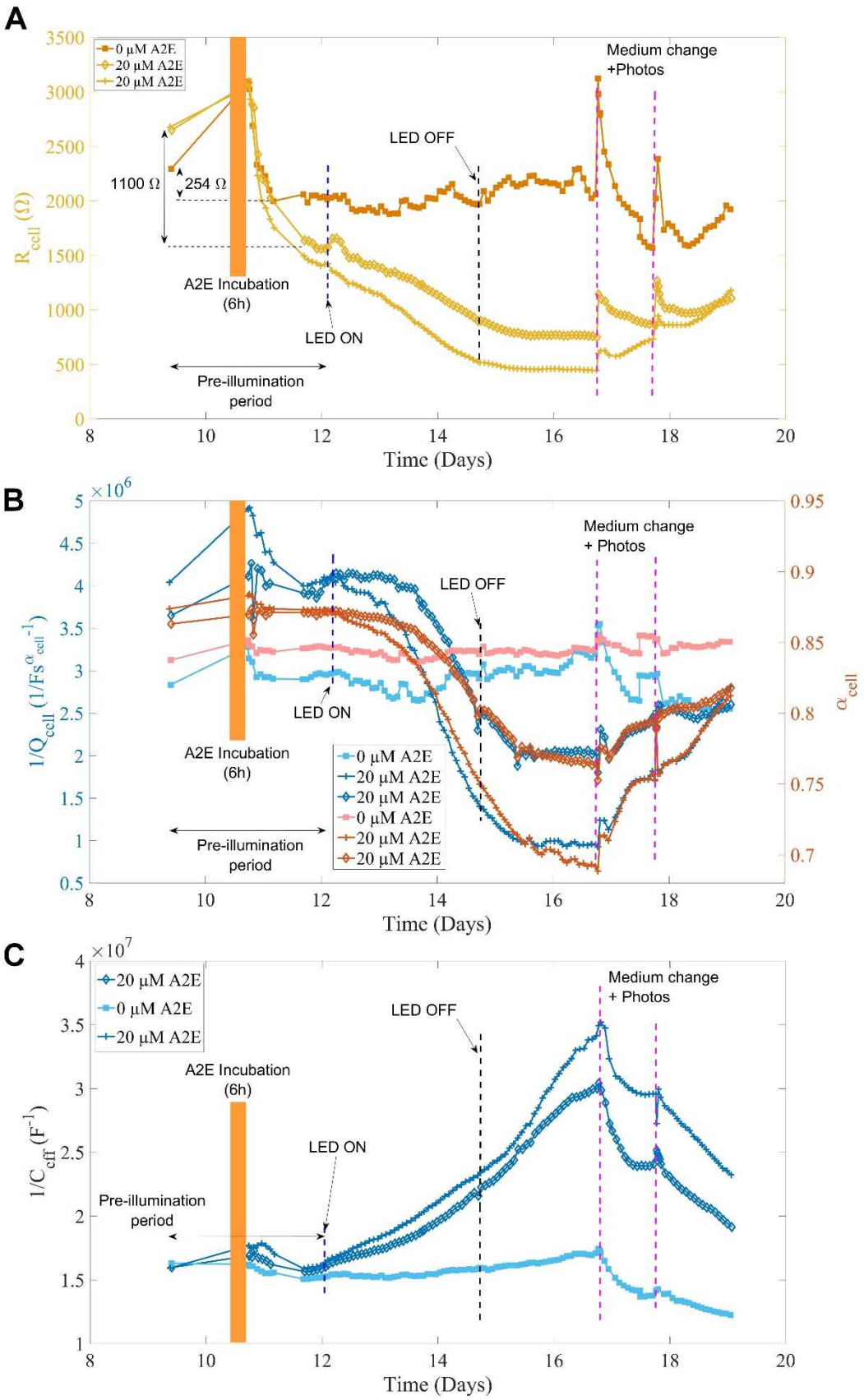

Figure 6 Variations of R_{cell} (A), cell layer CPE parameters (B) and $1/C_{eff}$ (C) after A2E incubation (indicated by the orange bar), during 430 nm blue light exposure (after LED ON label) and after blue light exposure (after LED OFF label). A2E concentration: 0 µM (squares), 20 µM (cross and diamond).

4. Discussion

In this work, the retinal pigment epithelium cultured on top of platinum electrodes is studied using impedance spectroscopy. A dedicated electrical circuit model is developed using a CPE associated with a reconstructed effective capacitance of the cell layer. It has been shown that in the case of two different disruptions of the cell layer, namely EDTA and electric pulse perturbations, the $1/Q_{cell}$ and α_{cell} parameters of the CPE remain correlated. This supports the fact that the CPE parameter variation has only one physical origin which rules the variation of both $1/Q_{cell}$ and α_{cell} at the same time. The spatial distribution of phospholipids dipolar moment is assumed to be the cause of this variation. Also, similar to what has been previously described in [27] [26] for the case of the electrode-electrolyte interface, a capacitance has been reconstructed from the other parameters of the model and defined as the average capacitance. This capacitance would be the CPE parameter Q_{cell} if the α_{cell} parameter was equal to one. This also shows that the connection between the parameters $1/Q_{cell}$ and α_{cell} of the CPE is not specific to the electrode-electrolyte interface. However, and even if it is involved in the C_{eff} construction, the R_{cell} parameter can vary independently from the $(1/Q_{cell}, \alpha_{cell})$ couple. Indeed, it can decrease before (EDTA assay) or after (pulse assay) with respect to the $(1/Q_{cell}, \alpha_{cell})$ couple, thus showing independence between the two parameters R_{cell} and $1/Q_{cell}$. Therefore, it can be considered that the variations of R_{cell} reflect another characteristic of the cell layer: the barrier's strength of the epithelium accomplished by the tight junctions. From that point of view, one last assay is performed on the same device as an application using A2E and blue light for the cell layer perturbation.

The shinning of blue light on A2E is known to generate species that damage mitochondria and cell membranes [7]. The delays measured on parameter stabilization observed after blue light exposure is likely due to an accumulation of such species in the cell culture medium and in the intracellular medium, resulting in damages to the layer even after light exposure has been stopped. Upon culture medium replacement, the parameters of the chambers that received A2E move toward their previous values indicating that the cell layer is not completely destroyed and that it can grow again.

Furthermore, R_{cell} variation is observed in the pre-illumination period, for the chambers that received A2E but haven't received light yet. Thanks to the previous EDTA and pulse tests we are assuming that the R_{cell} parameter is linked to the cell's tight junction. Therefore, it is proposed that A2E has an intrinsic effect on the cells tight junctions, while the blue light exposure on A2E loaded cells is the cause of a more profound damage of the cell layer, involving membrane destruction.

5. Conclusion

In this study of retinal pigment epithelium cells based on bio-impedance measurements, a setup measuring automatically the impedance spectra has been constructed, and an equivalent circuit model has been presented. The parameter variation of this model has been analyzed with respect to two controlled assays targeting specific elements of the cell layer. From those assays it has been concluded that the R_{cell} parameter is associated with the cell layer tight junctions while C_{eff} and the $(1/Q_{cell},\ \alpha_{cell})$ couple can be associated with the cells membranes. However, both $1/Q_{cell}$ and α_{cell} parameters have been considered to represent the same physical characteristic of the cell layer: the spatial distribution of the phospholipid's dipolar moments. Based on this analysis of the biophysical significance of the parameters of the model, an experiment involving A2E and blue light exposure of the cell layer have been performed. The monitoring and analysis of the impedance parameter variation during the blue light exposure permit to conclude: 1. the A2E itself has an effect on the cell layer's tight junction 2. the shinning of blue light on A2E loaded cells is inducing cell layer destruction that can be followed in real time and in the incubator's environment. This approach of cell state analysis using impedance spectroscopy offers non-invasive and non-destructive measurements. It can be adapted to a wide range of biological tissues in-vitro. It can also be adapted on in-vivo studies or implants (given the fact that macro-electrodes such as the one in this paper are used). This way it is possible to monitor not only the state of the interface between the implant and the tissue but also the tissue itself.

Acknowledgment

Jocelyn Boutzen acknowledges support from Ecole Normale Supérieure Paris-Saclay scholarship. The authors acknowledge support from ESIEE Paris (Noisy-le-Grand) and the Vision Institute (Paris). The authors thank Diep Nguyen for English proofreading.

6. Bibliography

[1] G.-Y. Sui, G.-C. Liu, G.-Y. Liu, Y.-Y. Gao, Y. Deng, W.-Y. Wang, S.-H. Tong et L. Wang, *British Journal of Ophthalmology,* vol. 97, pp. 389-394, 2013.

[2] J. R. Sparrow, K. Nakanishi et C. A. Parish, *Investigative Ophthalmology & Visual Science,* vol. 41, pp. 1981-1989, 6 2000.

[3] R. S. Ramrattan, T. L. Schaft, C. M. Mooy, W. C. Bruijn, P. G. Mulder et P. T. Jong, *Investigative Ophthalmology & Visual Science,* vol. 35, pp. 2857-2864, 5 1994.

[4] C. K. Dorey, G. Wu, D. Ebenstein, A. Garsd et J. J. Weiter, *Investigative Ophthalmology & Visual Science,* vol. 30, pp. 1691-1699, 8 1989.

[5] O. Strauss, *Physiological Reviews,* vol. 85, pp. 845-881, 2005.

[6] S. Erik G Nilsson, S. P Sundelin, U. Wihlmark et U. T Brunk, *Documenta ophthalmologica. Advances in ophthalmology,* vol. 106, pp. 13-6, 2 2003.

[7] M. Marie, K. Bigot, C. Angebault, C. Barrau, P. Gondouin, D. Pagan, S. Fouquet, T. Villette, J.-A. Sahel, G. Lenaers et S. Picaud, *Cell Death & Disease,* vol. 9, p. 287, 2 2018.

[8] U. Wihlmark, A. Wrigstad, K. Roberg, S. E. G. Nilsson et U. T. Brunk, *Free Radical Biology and Medicine,* vol. 22, pp. 1229-1234, 1997.

[9] B. S. Winkler, M. E. Boulton, J. D. Gottsch and P. Sternberg, *Molecular vision,* vol. 5, pp. 32-32, 11 1999.

[10] J. T. S. Irvine, D. C. Sinclair et A. R. West, *Adv. Mater.,* vol. 2, pp. 132-138, 6 2019.

[11] R. Ehret, W. Baumann, M. Brischwein, A. Schwinde et B. Wolf, *Medical and Biological Engineering and Computing,* vol. 36, pp. 365-370, 01 5 1998.

[12] V. Savolainen, K. Juuti-Uusitalo, N. Onnela, H. Vaajasaari, S. Narkilahti, R. Suuronen, H. Skottman et J. Hyttinen, *Annals of Biomedical Engineering,* vol. 39, p. 3055, 9 2011.

[13] J. R. Macdonald, *Annals of Biomedical Engineering,* vol. 20, pp. 289-305, 01 5 1992.

[14] E. Barsoukov et J. R. Macdonald, John Wiley & Sons, 2018.

[15] A. Soley, M. Lecina, X. Gámez, J. J. Cairó, P. Riu, X. Rosell, R. Bragós et F. Gòdia, *Journal of Biotechnology,* vol. 118, pp. 398-405, 2005.

[16] M. Pavlin, M. Kanduser, M. Rebersek, G. Pucihar, F. X. Hart, R. Magjarevic and D. Miklavcic, *Biophysical journal,* vol. 88, pp. 4378-4390, 6 2005.

[17] D. Holmes, D. Pettigrew, C. H. Reccius, J. D. Gwyer, C. Berkel, J. Holloway, D. E. Davies et H. Morgan, *Lab Chip,* vol. 9, n° %120, pp. 2881-2889, 2009.

[18] W. Gamal, S. Borooah, S. Smith, I. Underwood, V. Srsen, S. Chandran, P. O. Bagnaninchi and B. Dhillon, *Biosensors & bioelectronics,* vol. 71, pp. 445-455, 9 2015.

[19] J. Yeste, M. García-Ramírez, X. Illa, A. Guimerà, C. Hernández, R. Simó et R. Villa, *Lab Chip,* vol. 18, n° %11, pp. 95-105, 2018.

[20] J. Wegener, C. R. Keese et I. Giaever, *Experimental Cell Research,* vol. 259, pp. 158-166, 2000.

[21] J. Wegener, M. Sieber et H.-J. Galla, *Journal of Biochemical and Biophysical Methods,* vol. 32, pp. 151-170, 1996.

[22] J. C. Williams, J. A. Hippensteel, J. Dilgen, W. Shain et D. R. Kipke, *Journal of Neural Engineering,* vol. 4, pp. 410-423, 11 2007.

[23] K.-K. Lee, J. He, A. Singh, S. Massia, G. Ehteshami, B. Kim et G. Raupp, *Journal of Micromechanics and Microengineering,* vol. 14, pp. 32-37, 8 2003.

[24] B. Srinivasan, A. R. Kolli, M. B. Esch, H. E. Abaci, M. L. Shuler and J. J. Hickman, *Journal of laboratory automation,* vol. 20, pp. 107-126, 4 2015.

[25] O. Y. F. Henry, R. Villenave, M. J. Cronce, W. D. Leineweber, M. A. Benz et D. E. Ingber, *Lab on a chip,* vol. 17 13, pp. 2264-2271, 2017.

[26] P. Córdoba-Torres, T. J. Mesquita, O. Devos, B. Tribollet, V. Roche et R. P. Nogueira, *Electrochimica Acta,* vol. 72, pp. 172-178, 2012.

[27] G. J. Brug, A. L. G. Eeden, M. Sluyters-Rehbach et J. H. Sluyters, *Journal of Electroanalytical Chemistry and Interfacial Electrochemistry,* vol. 176, pp. 275-295, 1984.

[28] Y. Ando, K. Mizutani et N. Wakatsuki, *Journal of Food Engineering,* vol. 121, pp. 24-31, 2014.

[29] M. L. Yarmush, A. Golberg, G. Serša, T. Kotnik et D. Miklavčič, *Annual Review of Biomedical Engineering,* vol. 16, pp. 295-320, 2014.

[30] E. Arnault, C. Barrau, C. Nanteau, P. Gondouin, K. Bigot, F. Viénot, E. Gutman, V. Fontaine, T. Villette, D. Cohen-Tannoudji, J.-A. Sahel et S. Picaud, *PLOS ONE,* vol. 8, pp. 1-12, 8 2013.

[31] P. Córdoba-Torres, T. J. Mesquita et R. P. Nogueira, *J. Phys. Chem. C,* vol. 119, pp. 4136-4147, 2015.

[32] B. Hirschorn, M. E. Orazem, B. Tribollet, V. Vivier, I. Frateur et M. Musiani, *Electrochimica Acta,* vol. 55, pp. 6218-6227, 2010.

[33] K. A. Rezai, A. Lappas, L. Kohen, P. Wiedemann et K. Heimann, *Graefe's Archive for Clinical and Experimental Ophthalmology,* vol. 235, pp. 48-55, 01 1 1997.